ACADEMIC
PRESS

Available online at www.sciencedirect.com
SCIENCE DIRECT®

Journal of Solid State Chemistry 172 (2003) 305–318

JOURNAL OF
SOLID STATE
CHEMISTRY

http://elsevier.com/locate/jssc

Synthesis and crystal structure of new uranyl tungstates $M_2(UO_2)(W_2O_8)$ (M = Na, K), $M_2(UO_2)_2(WO_5)O$ (M = K, Rb), and $Na_{10}(UO_2)_8(W_5O_{20})O_8$

S. Obbade,[a,*] C. Dion,[a] E. Bekaert,[a] S. Yagoubi,[a] M. Saadi,[b] and F. Abraham[a]

[a] *Laboratoire de Cristallochimie et Physicochimie du Solide, UMR CNRS 8012, ENSCL-USTL, BP 108, 59652 Villeneuve d'Ascq Cedex, France*
[b] *Laboratoire de Chimie de Coordination et Analytique, Faculté des Sciences, Université Chouaib Doukkali, B.P. 20, El Jadida, Morocco*

Received 6 November 2002; received in revised form 27 January 2003; accepted 31 January 2003

Abstract

The solid-state reactions of UO_3 and WO_3 with M_2CO_3 (M = Na, K, Rb) at 650°C for 5 days result, accordingly the starting stoichiometry, in the formation of $M_2(UO_2)(W_2O_8)$ (M = Na (**1**), K (**2**)), $M_2(UO_2)_2(WO_5)O$ (M = K (**3**), Rb (**4**)), and $Na_{10}(UO_2)_8(W_5O_{20})O_8$ (**5**). The crystal structures of compounds **2**, **3**, **4**, and **5** have been determined by single-crystal X-ray diffraction using Mo($K\alpha$) radiation and a charge-coupled device detector. The crystal structures were solved by direct methods and Fourier difference techniques, and refined by a least-squares method on the basis of F^2 for all unique reflections. For (**1**), unit-cell parameters were determined from powder X-ray diffraction data. Crystallographic data: **1**, monoclinic, $a = 12.736(4)$ Å, $b = 7.531(3)$ Å, $c = 8.493(3)$ Å, $\beta = 93.96(2)°$, $\rho_{cal} = 6.62(2)\ g/cm^3$, $\rho_{mes} = 6.64(1)\ g/cm^3$, $Z = 4$; **2**, orthorhombic, space group $Pmcn$, $a = 7.5884(16)$ Å, $b = 8.6157(18)$ Å, $c = 13.946(3)$ Å, $\rho_{cal} = 6.15(2)\ g/cm^3$, $\rho_{mes} = 6.22(1)\ g/cm^3$, $Z = 8$, $R1 = 0.029$ for 80 parameters with 1069 independent reflections; **3**, monoclinic, space group $P2_1/n$, $a = 8.083(4)$ Å, $b = 28.724(5)$ Å, $c = 9.012(4)$ Å, $\beta = 102.14(1)°$, $\rho_{cal} = 5.83(2)\ g/cm^3$, $\rho_{mes} = 5.90(2)\ g/cm^3$, $Z = 8$, $R1 = 0.037$ for 171 parameters with 1471 reflections; **4**, monoclinic, space group $P2_1/n$, $a = 8.234(1)$ Å, $b = 28.740(3)$ Å, $c = 9.378(1)$ Å, $\beta = 104.59(1)°$, $\rho_{cal} = 6.13(2)\ g/cm^3$, $\rho_{mes}=6.19(3)\ g/cm^3$, $Z = 8$, $R1 = 0.037$ for 171 parameters with 1452 reflections; **5**, monoclinic, space group $C2/c$, $a = 24.359(5)$ Å, $b = 23.506(5)$ Å, $c = 6.8068(14)$ Å, $\beta = 94.85(3)°$, $\rho_{cal} = 6.42(2)\ g/cm^3$, $\rho_{mes}=6.39(3)\ g/cm^3$, $Z = 8$, $R1 = 0.036$ for 306 parameters with 5190 independent reflections. The crystal structure of **2** contains linear one-dimensional chains formed from edge-sharing UO_7 pentagonal bipyramids connected by two octahedra wide (W_2O_8) ribbons formed from two edge-sharing WO_6 octahedra connected together by corners. This arrangement leads to $[UW_2O_{10}]^{2-}$ corrugated layers parallel to (001). Owing to the unit-cell parameters, compound **1** probably contains similar sheets parallel to (100). Compounds **3** and **4** are isostructural and the structure consists of bi-dimensional networks built from the edge- and corner-sharing UO_7 pentagonal bipyramids. This arrangement creates square sites occupied by W atoms, a fifth oxygen atom completes the coordination of W atoms to form WO_5 distorted square pyramids. The interspaces between the resulting $[U_2WO_{10}]^{2-}$ layers parallel to $(10\bar{1})$ plane are occupied by K or Rb atoms. The crystal structure of compound **5** is particularly original. It is based upon layers formed from UO_7 pentagonal bipyramids and two edge-shared octahedra units, W_2O_{10}, by the sharing of edges and corners. Two successive layers stacked along the [100] direction are pillared by WO_4 tetrahedra resulting in sheets of double layers. The sheets are separated by Na^+ ions. The other Na^+ ions occupy the rectangular tunnels created within the sheets. In fact complex anions $W_5O_{20}^{10-}$ are built by the sharing of the four corners of a WO_4 tetrahedron with two W_2O_{10} dimmers, so, the formula of compound **5** can be written $Na_{10}(UO_2)_8(W_5O_{20})O_8$.

---

1. Introduction

During these last decades, the uranyl compounds have received a great and particular attention in solid-state chemistry owing to their very important environmental aspect and the possibility of their applications in medicine and in the nuclear industry. The association of uranyl ion with transition metal oxoanions (V, Nb, Mo, W,...) [1–12], carbonate, nitrate, phosphate, sulfate,... [13–18] allowed the synthesis of several compounds with complex and varied crystal structures.

In uranyl materials, the UO_2^{2+} ion can be coordinated in the equatorial plane by four, five or six anions

---

[*] Corresponding author. Fax: 33-320-436-814.
E-mail address: obbade@ensc-lille.fr (S. Obbade).

doi:10.1016/S0022-4596(03)00103-8

Table 1
Unit-cell parameters (Å) refined from powder X-ray data, figures of merit, and calculated and measured densities (g/cm^3) for compounds (**1**), (**2**), (**3**), (**4**), and (**5**)

Compounds	Cell parameters	F_{20}	ρ_{cal}	ρ_{mes}
$Na_2(UO_2)W_2O_8$	$a = 12.736(4)$ $b = 7.531(3)$ $c = 8.493(3)$ $\beta = 93.96(2)$	29.03 (53, 0.013)	6.62(2)	6.64(1)
$K_2(UO_2)W_2O_8$	$a = 7.585(1)$ $b = 8.612(1)$ $c = 13.956(2)$	57.14 (35, 0.010)	6.15(2)	6.22(1)
$K_2(UO_2)_2(WO_5)O$	$a = 8.084(2)$ $b = 28.731(7)$ $c = 9.010(2)$ $\beta = 102.16(2)$	26.14 (45, 0.017)	5.83(2)	5.90(2)
$Rb_2(UO_2)_2(WO_5)O$	$a = 8.237(2)$ $b = 28.744(8)$ $c = 9.377(2)$ $\beta = 104.59(2)$	29.49 (39, 0.018)	6.13(2)	6.19(3)
$Na_{10}(UO_2)_8(W_5O_{20})O_8$	$a = 24.356(4)$ $b = 23.507(4)$ $c = 6.804(1)$ $\beta = 94.86(1)$	08.33 (240, 0.010)	6.42(2)	6.39(3)

forming octahedron, pentagonal bipyramid or hexagonal bipyramid, respectively, the pentagonal bipyramid coordination being the most common mode of accommodation of uranyl ion. The other elements (M = V, Nb, Mo, W, P, S,…), notably in the highest oxidation state, form tetrahedral MO_4, square pyramidal MO_5 or octahedral MO_6 entities. They can act as bridging coordination modes to connect together uranyl polyhedra or clusters formed by edge or corner-shared uranyl polyhedra. Numerous arrangements of UO_x ($x = 6$, 7, 8) and MO_n ($n = 4$, 5, 6) can be obtained giving rise to low-dimensional architectures or open-framework structures. The size of the alkali or the alkaline earth cations has also an effect on the type of network that forms. In numerous compounds, a layered structure is obtained, where the interlayer spaces are occupied by the mono or divalent cations. So, this tendency to form layered structures, confers to these materials remarkable properties in the domains of insertion, exchanges and electrical ionic conductivity due to interlayer cations mobility. For example, hydrogen uranyl phosphate tetrahydrate $HUO_2PO_4 \cdot 4H_2O$ (HUP) has been shown to have the best selective proton conductivity at room temperature and has received particular attention because of its potential applications in electrochemical systems [19–22].

Recently, we have reported several layered uranyl vanadates [3–5,9]. In a preliminary communication [10], we have also reported the synthesis and crystal structure investigations of some uranyl vanadates, molybdates and tungstates of alkali metals.

The present paper is dealing with the synthesis and the crystal structure of new uranyl tungstates of sodium, potassium and rubidium in which the tungsten atom adopts different coordination geometries giving rise to four-coordinated WO_4 tetrahedra, five-coordinated WO_5 square pyramids and six-coordinated WO_6 octahedra leading to three different new arrangements.

2. Experimental

2.1. Powder samples preparation and crystal growth

The starting materials, M_2CO_3 (M = Na K, Rb) (Aldrich), WO_3 (Prolabo) and U_3O_8 (Prolabo), were used as received. Pure powder samples of the five compounds were prepared by solid-state reactions. For each sample, mixed starting materials in the appropriate stoichiometries were thoroughly mixed and were heated at 650°C in air for 5 days with intermediate grindings. The end of the reaction and the purity of the synthesized products were confirmed by X-ray diffraction using a Guinier–De Wolff camera and Cu$K\alpha$ radiation.

Transparent yellow single crystals of **1** and **2** were obtained by heating the powder samples in air in

Table 2
Crystal data, intensity collection, and structure

(a) Refinement parameters for $M_2(UO_2)_2(WO_5O$, M = K, Rb (**3**) and (**4**)

	$K_2(UO_2)_2(WO_5)O$		$Rb_2(UO_2)_2(WO_5)O$	
Crystal data				
Chemical formula weight	898.11 g/mol		990.85 g/mol	
Crystal symmetry	Monoclinic		Monoclinic	
Space group	$P21/n$		$P21/n$	
Unit cell refined from single-crystal data	$a = 8.083(4)$ Å		8.234(1) Å	
	$b = 28.724(5)$ Å		28.740(3) Å	
	$c = 9.012(4)$ Å		9.378(1) Å	
	$\beta = 102.14(1)°$		104.59(1)°	
	$V = 2045.5(1)$ Å^3		2147.7(1) Å^3	
Z	8		8	
Data collection				
Temperature (K)	293(2)		293(2)	
Equipment	Bruker SMART CCD		Bruker SMART CCD	
Radiation Mo$K\alpha$ (Å)	0.71073		0.71073	
Scan mode	ω		ω	
Recording angular range (°)	2.67–23.35		2.65–23.33	
Recording reciprocal space	$-7 \leqslant h \leqslant 8$		$-9 \leqslant h \leqslant 9$	
	$-23 \leqslant k \leqslant 32$		$-31 \leqslant k \leqslant 30$	
	$-10 \leqslant l \leqslant 9$		$-10 \leqslant l \leqslant 10$	
No. of measured reflections	3897		5651	
No. of independent reflections	1471		1452	
μ (cm^{-1}) (for $\lambda_{K\alpha}$ = 0.71073 Å)	436.56		498.11	
Limiting faces and distances (mm)	$1\ 0\ \bar{1}$	0.019	$\bar{3}\ \bar{3}\ \bar{5}$	0.055
From an arbitrary origin	$\bar{1}\ 0\ 1$	0.003	$3\ 3\ 5$	0.045
	$0\ 1\ 0$	0.023	$0\ 1\ 0$	0.019
	$0\ \bar{1}\ 0$	0.027	$0\ \bar{1}\ 0$	0.011
	$0\ 0\ 1$	0.061	$\bar{2}\ 1\ 2$	0.018
	$0\ 0\ \bar{1}$	0.051	$2\ \bar{1}\ \bar{2}$	0.017
R merging factor	0.075		0.067	
Refinement				
Refined parameters/restraints	171/0		171/0	
Goodness-of-fit on F_2	1.20		1.05	
$R_1[I > 2\sigma(I)]$	0.037		0.037	
$wR_2[I > 2\sigma(I)]$	0.075		0.082	
R_1 for all data	0.039		0.038	
wR_2 for all data	0.075		0.083	
Largest diffraction peak and hole (e/Å^3)	2.27 to −2.85		3.85 to −1.89	

(b) Refinement parameters for $K_2(UO_2)W_2O_8$ (2) and $Na_{10}(UO_2)_8(W_5O_{20})O_8$ (5)

	$K_2(UO_2)W_2O_8$	$Na_{10}(UO_2)_8(W_5O_{20})O_8$
Crystal data		
Chemical formula weight	843.93 g/mol	3757.39 g/mol
Crystal symmetry	Orthorhombic	Monoclinic
Space group	$Pmcn$	$C2/c$
Unit cell from single-crystal data	$a = 7.5884(16)$ Å	24.359(5) Å
	$b = 8.6157(18)$ Å	23.506(5) Å
	$c = 13.946(3)$ Å	6.8068(14) Å
		94.85(3)
	$V = 911.8(3)$ Å^3	3883.5(1) Å^3
Z	4	4
Data collection		
Temperature (K)	293(2)	293(2)
Equipment	Bruker SMART CCD	Bruker SMART CCD
Radiation Mo$K\alpha$ (Å)	0.71073	0.71073
Scan mode	ω	ω
Recording angular range (°)	2.58–29.30	1.21–31.51

Table 2 (*continued*)

(b) Refinement parameters for $K_2(UO_2)W_2O_8$ (2) and $Na_{10}(UO_2)_8(W_5O_{20})O_8$ (5)

Recording reciprocal space	$-10 \leqslant h \leqslant 10$		$-35 \leqslant h \leqslant 34$	
	$-11 \leqslant k \leqslant 11$		$-33 \leqslant k \leqslant 34$	
	$-18 \leqslant l \leqslant 18$		$-9 \leqslant l \leqslant 9$	
No. of measured reflections	5261		17761	
No. of independent reflections	1069		5190	
μ (cm^{-1}) (for $\lambda_{K\alpha}$=0.71073 Å)	438.37		482.03	
Limiting faces and distances (mm)	1 0 0	0.075	1 0 0	0.006
From an arbitrary origin	$\bar{1}$ 0 0	0.111	$\bar{1}$ 0 0	0.015
	0 1 0	0.059	0 1 0	0.085
	0 $\bar{1}$ 0	0.025	0 $\bar{1}$ 0	0.016
	0 0 1	0.014	0 0 1	0.17
	0 0 $\bar{1}$	0.024	0 0 $\bar{1}$	0.18
R merging factor	0.050		0.049	
Refinement				
Refined parameters/restraints	80/0		306/0	
Goodness-of-fit on F^2	1.08		1.04	
$R_1[I>2\sigma(I)]$	0.029		0.036	
$wR_2[I>2\sigma(I)]$	0.062		0.081	
R_1 for all data	0.035		0.041	
wR_2 for all data	0.064		0.084	
Largest diffraction peak and hole(e/Å^3)	1.81 to −2.56		3.99 to −4.39	

$R_1 = \sum(|F_o| - |F_c|)/\sum|F_o|$

$wR_2 = \left[\sum w(F_o^2 - F_c^2)^2/\sum w(F_o^2)^2\right]^{1/2}$

$w = 1/[\sigma^2(F_o^2) + (aP)^2 + bP]$ where a and b are refinable parameters and $P = (F_o^2 + 2F_c^2)/3$.

Table 3
Atomic coordinates and equivalent displacement parameters (Å^2) for $K_2(UO_2)W_2O_8$ (**2**)

Atom	*x*	*y*	*z*	U_{eq} (Å^2)
U	0.25	0.52721(5)	0.49618(4)	0.0104(1)
W	0.00175(5)	0.85444(4)	0.42732(3)	0.0114(1)
K1	−0.25	0.1508(4)	0.3064(2)	0.0189(7)
K2	0.25	0.1715(4)	0.2827(3)	0.0310(8)
O1	−0.0290(8)	0.6508(7)	0.4844(6)	0.0167(15)
O2	−0.25	0.8676(10)	0.4172(7)	0.0136(19)
O3	0.0353(8)	1.0652(7)	0.4224(5)	0.0121(13)
O4	0.25	0.8081(10)	0.4668(7)	0.0147(20)
O5	0.0329(9)	0.8087(8)	0.3077(5)	0.0202(16)
O6	0.25	0.5559(10)	0.6247(7)	0.0179(21)
O7	0.25	0.4934(10)	0.3680(7)	0.0174(21)

Note: The anisotropic displacement factor exponent takes the form $-2\pi^2[h^2a*^2\,U_{11} + \cdots + 2hka*b*U_{12}]$ and $U_{eq} = 1/3(\sum_i \sum_j U_{ij}a*_i\,a*_j\,a_i a_j)$.

platinum crucibles just above the non-congruent melting temperature, 850°C and 750°C, respectively, during 1 h and slow cooling at a rate of 5°C/h to room temperature. Unfortunately, in spite of numerous efforts, the obtained single crystals of **1** were not good enough for a crystal structure study.

When the powder samples corresponding to **1** and **2** are heated widely above the melting point, typically 100°C above, the results were a mixture of two types of single crystals, yellow crystals of **1** or **2** and orange-colored single crystals corresponding to compounds **5** and **3**, respectively.

Transparent orange-colored single crystals of compound **3** were also prepared in a K_2CO_3 flux using a mixture U_3O_8/WO_3 of molar ratio 0.67/1 in a five-fold excess of K_2CO_3. The sample was thoroughly mixed in a platinum crucible, heated at 950°C during 60 h and slowly cooled at a rate of 5°C/h to room temperature. Single crystals of **4** were grown under the same conditions using Rb_2CO_3 instead of K_2CO_3 as flux.

For each case, the presence of the metal elements Na/K/Rb, U and W in the prepared crystals was confirmed by energy dispersive spectroscopy analysis (EDS) using a JEOL JSM-5300 Scanning Microscope.

2.2. Crystal structure determination

Crystals of **2**, **3**, **4** and **5** with the dimensions 0.180 mm × 0.084 mm × 0.038 mm, 0.112 mm × 0.088 mm × 0.022 mm, 0.100 mm × 0.030 mm × 0.035 mm, and 0.350 mm × 0.103 mm × 0.021 mm, respectively, were selected, mounted on glass fibers and aligned on a Bruker SMART CCD X-ray diffractometer. Intensities were collected at room temperature using Mo$K\alpha$ ($\lambda = 0.71073$ Å) radiation selected by a graphite monochromator. The individual frames were measured using a ω-scan technique with an omega rotation of 0.3° and an acquisition time of 40 s per frame. After every data collection, the intensity data

Table 4
Atomic coordinates and isotropic or (equivalent for metal atoms) displacement parameters (Å^2) for $M_2(UO_2)_2(WO_5)O$ (M = K, Rb), (**3**) and (**4**)

	M = K				M = Rb			
Atom	x	y	z	$U_{iso}/U_{eq}*$	x	y	z	$U_{iso}/U_{eq}*$
U1	0.4724(2)	0.06715(4)	0.9686(2)	0.0135(4)*	0.4712(2)	0.06730(5)	0.9701(2)	0.0145(5)*
U2	0.6702(2)	0.16794(4)	1.2143(1)	0.0129(4)*	0.6643(2)	0.16789(5)	1.2181(2)	0.0128(4)*
U3	1.0917(2)	0.09874(4)	1.5756(2)	0.0160(4)*	0.0856(2)	0.09906(5)	0.5812(2)	0.0142(5)*
U4	0.3213(2)	0.18603(4)	0.8554(2)	0.0137(4)*	0.3153(2)	0.18640(5)	0.8616(2)	0.0121(5)*
W1	0.9110(2)	0.21038(4)	1.5460(2)	0.0137(4)*	0.9000(2)	0.21016(5)	1.5491(2)	0.0122(5)*
W2	0.7406(2)	0.03236(4)	1.3109(2)	0.0178(5)*	0.7348(2)	0.03188(5)	1.3114(2)	0.0182(5)*
M1	0.5890(12)	0.1217(2)	1.6069(9)	0.025(2)*	0.5814(5)	0.1211(1)	0.6090(5)	0.024(1)*
M2	0.9127(13)	0.2524(3)	1.9611(9)	0.039(3)*	0.3792(8)	0.2442(2)	1.4559(6)	0.057(2)*
M3	0.7301(12)	−0.0137(3)	1.6763(9)	0.045(3)*	0.2595(6)	0.0131(2)	1.3186(5)	0.038(1)*
M4	0.9854(13)	0.1020(3)	1.0121(9)	0.041(3)*	0.9773(7)	0.1011(2)	1.0195(6)	0.044(2)*
O1	0.509(3)	0.1650(6)	1.323(2)	0.002(5)	0.505(3)	0.1622(8)	1.312(3)	0.012(6)
O2	0.301(3)	0.0642(6)	1.072(2)	0.012(5)	0.316(3)	0.0632(8)	1.072(3)	0.018(7)
O3	0.844(3)	0.1750(6)	1.115(3)	0.016(6)	0.834(3)	0.1770(8)	1.132(3)	0.022(7)
O4	0.165(3)	0.1787(6)	0.968(3)	0.017(6)	0.169(3)	0.1785(8)	0.966(3)	0.014(7)
O5	0.461(3)	0.1969(7)	0.728(3)	0.014(6)	0.446(3)	0.1987(7)	0.745(3)	0.008(6)
O6	0.643(3)	0.0660(7)	0.859(3)	0.019(6)	0.637(4)	0.0684(9)	0.879(3)	0.035(8)
O7	0.869(3)	0.1528(7)	1.443(2)	0.011(5)	0.861(3)	0.1530(8)	1.450(3)	0.007(6)
O8	0.946(3)	0.0877(7)	1.693(3)	0.031(7)	−0.056(3)	0.0840(8)	0.691(3)	0.017(7)
O9	0.796(3)	0.2091(8)	1.685(3)	0.035(7)	0.781(3)	0.2082(9)	1.673(3)	0.026(7)
O10	0.612(3)	0.0451(8)	1.444(3)	0.035(7)	0.600(4)	0.0448(9)	1.426(3)	0.034(8)
O11	1.241(3)	0.1097(8)	1.455(3)	0.035(7)	0.220(3)	0.1122(8)	0.468(3)	0.016(7)
O12	1.293(3)	0.1089(7)	1.780(2)	0.016(6)	0.293(3)	0.1105(7)	0.782(3)	0.007(6)
O13	0.610(3)	0.0052(7)	1.135(3)	0.025(6)	0.605(3)	0.0065(9)	1.130(3)	0.033(8)
O14	0.764(3)	0.2347(7)	1.368(3)	0.018(6)	0.754(3)	0.2335(8)	1.370(3)	0.019(7)
O15	0.505(3)	0.1437(7)	1.013(3)	0.018(6)	0.505(3)	0.1439(8)	1.016(3)	0.018(7)
O16	0.680(3)	0.0874(7)	1.188(3)	0.024(6)	0.684(3)	0.0872(8)	1.189(3)	0.010(6)
O17	1.105(3)	0.1812(7)	1.638(3)	0.021(6)	1.102(3)	0.1814(8)	1.645(3)	0.018(7)
O18	1.013(3)	0.2680(7)	1.567(2)	0.017(6)	1.009(3)	0.2684(8)	1.563(3)	0.019(7)
O19	0.799(3)	−0.0276(7)	1.373(3)	0.027(6)	0.797(3)	−0.0272(9)	1.378(3)	0.029(8)
O20	0.952(3)	0.0551(7)	1.359(3)	0.031(7)	0.944(3)	0.0555(9)	1.376(3)	0.030(8)

Note: The anisotropic displacement factor exponent takes the form $-2\pi^2[h^2a*^2\,U_{11}+\cdots+2hka*b*U_{12}]$ and $U_{eq}=1/3(\sum_i\sum_j U_{ij}a*_i\,a*_j\,a_ia_j)$.

were reduced and corrected for Lorentz, polarization and background effects using the Bruker program SAINTPLUS [23]. Once the data processing was performed, the absorption corrections were computed by the Gaussian face-indexed method with the shape of the crystal using the program XPREP of the SHELXTL package [24] followed by SADABS program [25].

Powder X-ray diffraction data used for least-squares refinements of lattice parameters were recorded on a Siemens D5000 $\theta/2\theta$ diffractometer, at room temperature, using Bragg–Brentano geometry, with a back-monochromatized Cu$K\alpha$ radiation. Samples were very lightly ground and mounted on a flat sample plate. The diffraction pattern was scanned over the angle range 10–120° (2θ) in step of 0.03°(2θ) and a counting time of 10 s per step. The unit-cell parameters were refined by a least-squares procedure from the indexed powder diffraction pattern. Powder X-ray diffraction pattern and refined cell parameters with their figure of merit F_{20} defined by Smith and Snyder [26], are reported in Table 1. The density of each sample was measured with an automated Micromeritics Accupyc 1330 pycnometer using a 1-cm^3 cell and comparison with the calculated density gives integer values for the Z number of formula per unit cell (Table 1).

Crystal structures were determined in the centrosymmetric $Pmcn$ space group for **2**, $P2_1/n$ for **3** and **4** and $C2/c$ for **5** by direct methods using SHELXS program [27], which readily established the heavy atom positions (U, W, Rb and K). Oxygen atoms, and Na atoms for **5**, were localized from difference Fourier maps. The last cycles of refinement included atomic positions, anisotropic displacement parameters for all non-oxygen atoms, and anisotropic (compounds **1** and **2**) or isotropic (compounds **3** and **4**) displacement parameters for oxygen atoms. Full-matrix least-squares structure refinements against $|F^2|$ were carried out using the SHELXTL [24] package of programs. Some crystallographic final refinement details are given in Tables 2a and b. The final positional parameters and isotropic or equivalent atomic displacement parameters are presented in Table 3 for **2**, in Table 4 for **3** and **4** and in Table 5 for **5**. Additional crystallographic data are available on request upon the authors.

Table 5
Atomic coordinates and equivalent displacement parameters (Å^2) for $Na_{10}(UO_2)_8(W_5O_{20})O_8$ (**5**)

Atom	x	y	z	U_{eq}
U1	0.12684(1)	0.46655(1)	0.95523(5)	0.00972(8)
U2	0.12380(1)	0.37279(1)	0.48829(5)	0.01006(8)
U3	0.12707(2)	0.03289(1)	0.62564(5)	0.00990(8)
U4	0.12431(2)	0.12741(1)	1.09093(5)	0.00995(8)
W1	0.13177(2)	0.29932(1)	0.96725(5)	0.01030(9)
W2	0.13643(2)	0.20245(1)	0.62015(5)	0.01018(9)
W3	0	0.24593(2)	3/4	0.01637(9)
Na1	0.2506(2)	0.12062(19)	0.8151(7)	0.024(2)
Na2	0	0.3896(3)	3/4	0.027(2)
Na3	0	0.4508(3)	3/4	0.029(2)
Na4	0.2515(2)	−0.0442(2)	0.8276(7)	0.026(1)
Na5	0	0.1081(3)	3/4	0.025(1)
Na6	0	0.0483(3)	1.25	0.030(2)
Na7	0.2574(3)	0.2897(2)	0.7181(9)	0.045(2)
O1	0.1285(3)	0.2180(3)	0.9343(9)	0.014(1)
O2	0.0512(4)	0.4709(3)	0.9210(11)	0.021(2)
O3	0.2025(3)	0.4586(3)	0.9873(11)	0.018(2)
O4	0.1163(3)	0.3708(3)	0.8568(10)	0.015(2)
O5	0.1990(3)	0.1300(3)	1.1242(11)	0.018(2)
O6	0.0499(3)	0.3779(3)	0.4748(11)	0.018(2)
O7	0.1249(3)	0.2824(3)	0.6480(9)	0.015(2)
O8	0.0511(3)	0.0330(3)	0.6061(11)	0.020(2)
O9	0.0506(3)	0.1246(3)	1.0583(10)	0.019(2)
O10	0.2032(3)	0.0355(3)	0.6477(11)	0.019(2)
O11	0.1987(3)	0.3675(3)	0.5021(11)	0.019(2)
O12	0.1374(3)	0.4558(3)	0.6374(10)	0.016(2)
O13	0.1216(4)	0.4388(3)	1.2605(10)	0.020(2)
O14	0.0442(3)	0.2015(3)	0.6258(11)	0.020(2)
O15	0.1239(3)	0.1900(3)	0.3647(11)	0.019(2)
O16	0.1286(3)	−0.0442(3)	0.4457(10)	0.017(2)
O17	0.2034(3)	0.3042(3)	0.9861(11)	0.023(2)
O18	0.0401(3)	0.2906(3)	0.9113(11)	0.022(2)
O19	0.1280(3)	0.1300(3)	0.7249(10)	0.019(2)
O20	0.1252(4)	0.0604(3)	0.3168(9)	0.019(2)
O21	0.1193(4)	0.3114(3)	1.2138(10)	0.024(2)
O22	0.2081(3)	0.2061(3)	0.6393(11)	0.022(2)

Note: The anisotropic displacement factor exponent takes the form $-2\pi^2[h^2a*^2\,U_{11} + \cdots + 2hka*b*U_{12}]$ and $U_{eq} = 1/3(\sum_i \sum_j U_{ij}a*_i\,a*_j\,a_ia_j)$.

3. Crystal structure description and discussion

$M_2(UO_2)(W_2O_8)$ (M=Na (**1**), K (**2**)). The layered structure of **2** is built from an assemblage of UO_7 distorted pentagonal bipyramids and WO_6 octahedra. The UO_7 pentagonal bipyramids share opposite equatorial edges to form zig-zag infinite one polyhedron wide chains (UO_5) running along the *a*-axis. Two WO_6 octahedra shares an edge to form a dimeric unit W_2O_{10}. The dimeric units are corner-shared to form two octahedral wide ribbon (W_2O_8) running along the *a*-axis. The (W_2O_8) ribbons share edges with translationally equivalent (UO_5) chains, resulting in $(UW_2O_{10})^{2-}$ sheets parallel to (001) (Fig. 1). The tungsten uranyl layers are stacked along *c* and linked through bonds to K cations in the interlayer (Fig. 2). Owing to the resemblance of the two unit-cell parameters corresponding to the dimensions of the layers, one can assume that the Na compound **1** is probably built from the same $(UW_2O_{10})^{2-}$ corrugated layers parallel to (100), the differences in the ionic radius and coordination of Na^+ by oxygen atoms of the layers leading to a different stacking of the layers in the third direction.

The (UO_5) chains are common to many uranyl oxides, but the connection between chains by the two-octahedral wide ribbons is novel. In $USbO_5$ (28), UVO_5 [29–31], $U_2V_2O_{11}$ [32,33], $U_3V_2O_{14}\cdot 5H_2O$ (34) and $U_3P_2O_{14}\cdot 4H_2O$ [35] two successive chains are also deduced by a translation perpendicular to the chain direction. In $USbO_5$ [28] they are connected by a chain of corner-shared SbO_6 octahedra of one octahedron wide. Note that the (W_2O_8) ribbons in $K_2(UO_2)(W_2O_8)$ can also be described as two chains formed by corner-sharing WO_6 octahedra linked by the sharing of edges. In UVO_5 [29–31] (Fig. 3a), VO_5 square pyramids replace the SbO_6 octahedra. In $U_2V_2O_{11}$ [32,33], $U_3V_2O_{14}\cdot 5H_2O$ [34] and isostructural $U_3P_2O_{14}\cdot 4H_2O$ [35], the successive parallel chains are connected by VO_4 or PO_4 tetrahedra (Fig. 3b). In $U_2P_2O_{10}$ [36], more distorted (UO_5) chains are also linked by PO_4 tetrahedra in the same manner, in fact the chains are formed from two kinds of UO_7 bipyramids containing uranium atoms at oxidation states +4 and +6. In UMo_2O_8 [37] and α-U_3O_8 [38], two successive chains are translated parallel to their direction. In fact, the parallel chains are related by a mirror, so the non-shared oxygen atoms of the equatorial bases of UO_7 bipyramids are opposite. In UMo_2O_8 [37] they are connected by a two octahedra wide ribbon of MoO_6 octahedra linked only by corner-sharing, in fact in that compound the obtained layers are shared by corners to built a three-dimensional structure and the MoO_6 octahedra form a ReO_3-type slab of titled octahedra, two MoO_6 octahedra wide (Fig. 3c). In U_3O_8 [38], the chains are directly attached by corner-sharing, distorted hexagonal sites are produced between the chains, and U atoms in pentagonal bipyramidal coordination occupy them (Fig. 3d). In the recently published $M_6(UO_2)_5(VO_4)_2O_5$ with M=Na, K [9] and Rb [39], two types of behavior are simultaneously present, two strictly parallel chains are linked by tetrahedra as in $U_3V_2O_{14}\cdot 5H_2O$ [34], while two mirror-related chains are directly linked by corner-sharing as in U_3O_8 (Fig. 3e), depending on the chain distortion the uranium atoms occupying the created sites are in distorted octahedral or pentagonal bipyramidal coordination. Finally, in $U_2V_2O_{11}$ [32,33] they are linked by VO_4 tetrahedra to form flat layers (Fig. 3b), two parallel layers share an oxygen from VO_4 resulting in a three-dimensional framework and in the formation of corrugated layers in which (UO_5) chains are connected through V_2O_7 divanadate groups (Fig. 3f). Note that UVO_5 and $USbO_5$ compounds contain U^V and no

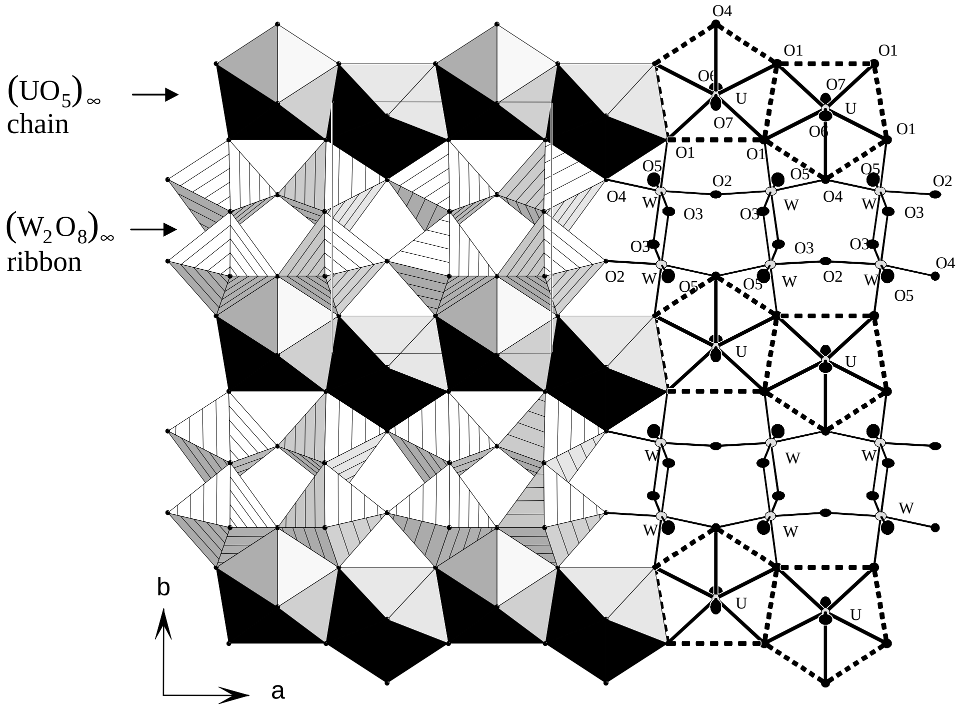

Fig. 1. Projection of the crystal structure of $K_2(UO_2)(W_2O_8)$ (**2**) on the (001) plane showing the connection between one-dimensional $(UO_5)_\infty$ chains consisting of edge-sharing distorted UO_7 pentagonal bipyramids and $(W_2O_8)_\infty$ ribbons consisting of W_2O_{10} dimeric units linked by corner-sharing.

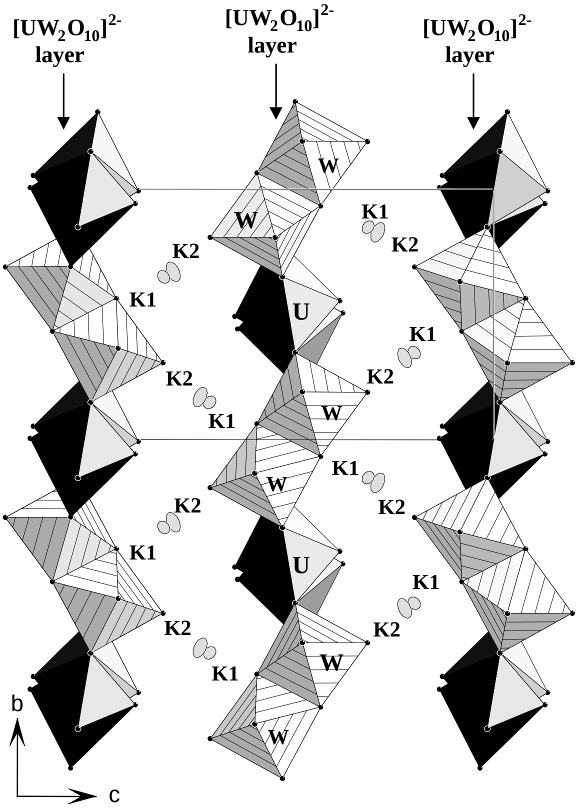

Fig. 2. Projection of the crystal structure of $K_2(UO_2)(W_2O_8)$ (**2**) on the (100) plane showing the corrugated $(UW_2O_{10})^{2-}$ layers stacked along the *c*-axis and the interlayer K atoms.

uranyl group is present and the layers are stacked by perpendicular chains containing –U–O–U–O– and –V–O–V–O– in UVO_5 and –U–O–Sb–O–U–O–Sb– in $USbO_5$. In both compounds, the U–O bond lengths along the chains perpendicular to the layers are greater than 2.0 Å. The structure of the infinite sheets can be described with the anion topologies, developed by Burns et al. [40,41] that contain only triangles, squares, and pentagons and are common to many borates, silicates, sulphates,….

Selected interatomic distances and bond valences for **2** are given in Table 6. There are two kinds of U–O distances in the flattened pentagonal bipyramid around U, two short bonds of 1.81(1) Å with a O–U–O angle of 178.6(4)° characteristic of the $[UO_2]^{2+}$ uranyl ion and five longer U–O distances (average value, 2.36(1) Å) forming the equatorial plane of the UO_7 bipyramids. The U–O bond lengths are in good accordance with the seven-fold coordination usually observed for U(VI) [42].

The WO_6 octahedron presents W–O distances ranging from 1.730(7) to 2.225(7) Å with an average value of 1.942 Å. The shortest W–O bond (1.730 Å) corresponds to O(5) oxygen non-shared with a UO_7 polyhedron. The tungsten atom is moved towards one O(3) oxygen atom of the bridge between two WO_6 octahedra (1.835 Å) and as a consequence is taken away from the other one (2.225 Å).

Bond valence sums calculations using Brown and Altermatt data [43] with $b = 0.37$ Å except for U–O

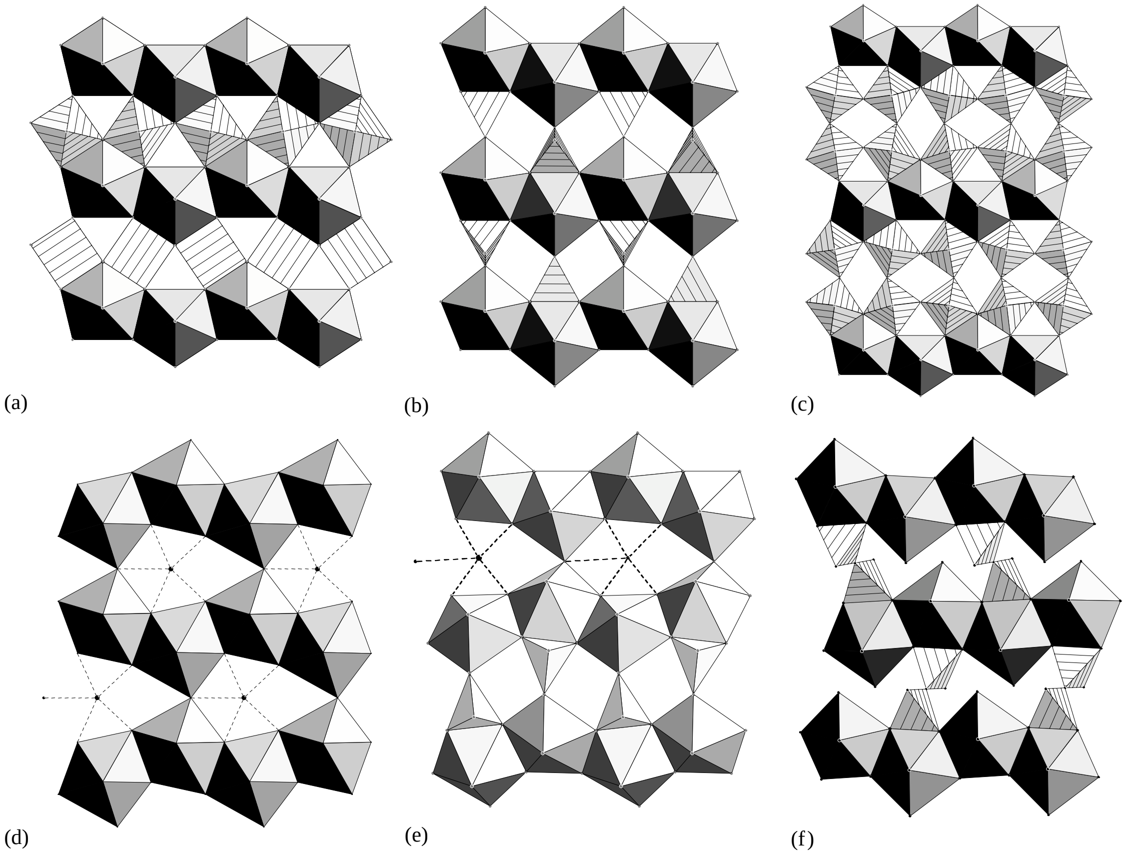

Fig. 3. The connection between $(UO_5)_\infty$ zig-zag chains consisting of UO_7 pentagonal bipyramids sharing opposite edges, (a) by SbO_6 octahedra or VO_5 square pyramids in U^{5+} containing compounds, $USbO_5$ and UVO_5, respectively, (b) by VO_4 or PO_4 tetrahedra in $U_3X_2O_{14}\cdot nH_2O$ (X = V, P), (c) by ReO_3-type slabs two octahedra wide in UMo_2O_8, (d) by corner-sharing in U_3O_8, (e) alternatively by VO_4 tetrahedra and by corner-sharing in $M_6(UO_2)_5(VO_4)_2O_5$ (M = Na, K, Rb) and (f) by divanate groups in $U_2V_2O_{11}$.

Table 6
Selected bond distances (Å) and bond valences for $K_2(UO_2)W_2O_8$ (**2**)

Atom	Distance	s_{ij}	Atom	Distance	s_{ij}
U–O6	1.809(9)	1.591	W–O5	1.730(7)	1.658
U–O7	1.811(9)	1.591	W–O3	1.835(6)	1.248
U–O1^{i}	2.289(6)	0.633	W–O2	1.919(1)	0.995
U–O1^{ii}	2.289(6)	0.633	W–O1	1.941(7)	0.937
U–O1^{iii}	2.376(6)	0.535	W–O4	2.003(3)	0.793
U–O1	2.376(6)	0.535	W–O3^{v}	2.225(7)	0.434
U–O4	2.455(9)	0.459			
Σs_{ij}		*5.977*	Σs_{ij}		*6.065*
K1–O5^{viii}	2.664(7)	0.237	K2–O3^{x}	2.700(7)	0.216
K1–O5^{ix}	2.664(7)	0.237	K2–O3^{xiii}	2.700(7)	0.216
K1–O6^{i}	2.704(9)	0.214	K2–O5^{ix}	2.756(7)	0.185
K1–O7^{ix}	2.785(9)	0.171	K2–O5^{xiv}	2.756(7)	0.185
K1–O3^{x}	2.801(7)	0.164	K2–O6^{xv}	2.949(9)	0.11
K1–O3^{xi}	2.801(7)	0.164	K2–O7	3.018(9)	0.091
K1–O2^{x}	2.888(9)	0.129	K2–O2^{ix}	3.260(9)	0.047
Σs_{ij}		*1.311*	Σs_{ij}		*1.05*

Symmetry codes: (i) $-x, 1-y, 1-z$; (ii) $0.5+x, 1-y, 1-z$; (iii) $0.5-x, y, z$; (iv) $1-x, 1-y, 1-z$; (v) $-x, 2-y, 1-z$; (vi) $x, 1+y, z$; (vii) $-x, 0.5+y, 0.5-z$; (viii) $-0.5+x, -0.5+y, 0.5-z$; (ix) $-x, -0.5+y, 0.5-z$; (x) $x, -1+y, z$; (xi) $-0.5-x, -1+y, z$; (xii) $-1+x, y, z$; (xiii) $0.5-x, -1+y, z$; (xiv) $0.5+x, -0.5+y, 0.5-z$; (xv) $x, 0.5-y, -0.5+z$.

bonds where the coordination independent parameters ($R_{ij} = 2.051$ Å, $b = 0.519$ Å) were taken from Burns et al. [40] provide values of 5.977, 6.065, 1.311 and 1.050 for U, W, K(1) and K(2), respectively. For the oxygen atoms the calculated valence bond sums range from 1.853 to 2.166 with an average value of 2.041.

*$M_2(UO_2)_2(WO_5)O$ (M = K (**3**), Rb (**4**)).* Compounds **3** and **4** are isostructural with 30 unique atoms (4 U, 2 W, 4 K or Rb and 20 O), all of which occupy general crystallographic positions (4e). The crystal structure of **3** and **4** is built from UO_7 pentagonal bipyramids and WO_5 square pyramids. The structure consists of layered arrangements of edge- and corner-shared UO_7 pentagonal bipyramids that can be considered as the primary building units. The pentagonal bipyramids for the four independent uranium atoms are associated by edge-sharing to form a tetrameric group U_4O_{21}. The three pentagonal bipyramids $U(1)O_7$, $U(2)O_7$ and $U(4)O_7$ are linked by the common corner O(15) and share the edges [O(15)–O(12)], [O(15)–O(16)], [O(15)–O(18)] to form a very dense cluster, the fourth pentagonal bipyramid $U(3)O_7$ is linked to $U(4)O_7$ through the [O(12)–O(17)] edge and with $U(1)O_7$ by O(12) corner to built the

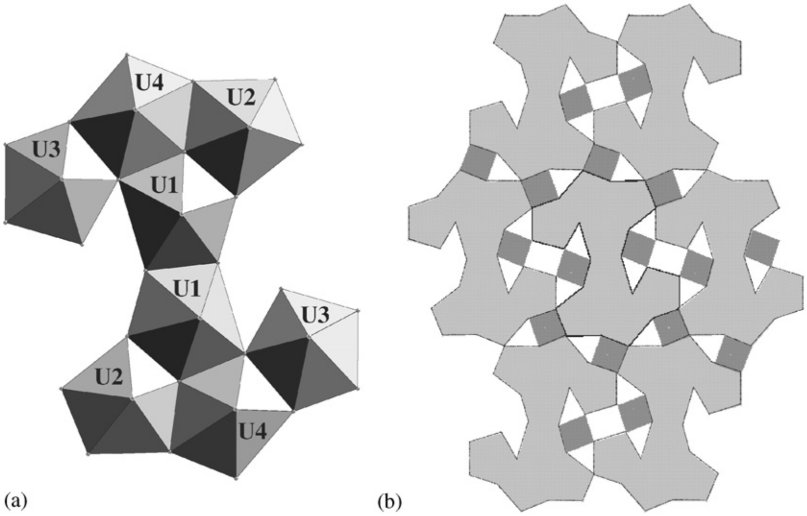

Fig. 4. (a) The SBU U_8O_{10} in $M_2(UO_2)_2(WO_5)O$ [M = K (**3**), Rb (**4**)] compounds consisting of edge-sharing distorted pentagonal bipyramids UO_7 and (b) the bi-dimensional arrangement of SBU showing the two types of sites occupied by WO_5 entities.

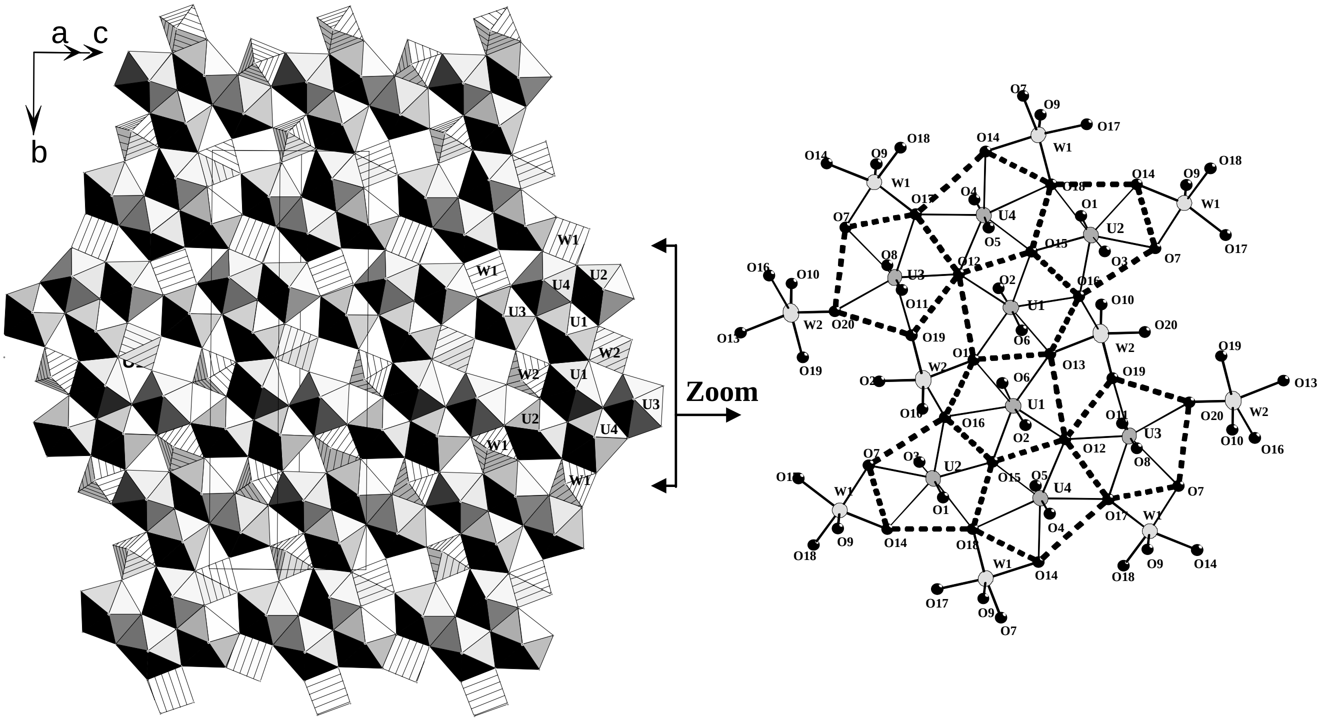

Fig. 5. Projection of the layer $(U_2WO_{10})^{2-}$ on the $(10\bar{1})$ plane of $M_2(UO_2)_2(WO_5)O$ [M = K (**3**), Rb (**4**)] compounds, showing the bi-dimensional arrangement of UO_7 pentagonal bipyramids and WO_5 square pyramids.

tetrameric unit. Dense clusters of edge-shared UO_7 pentagonal bipyramids occur in the structure of numerous uranyl-containing compounds. Two U_4O_{21} units related by an inversion center share a [O(13)–O(13)] edge to form the U_8O_{40} entity that constitutes the secondary building unit (SBU) of the bi-dimensional arrangement, Fig. 4. In fact the $U(1)O_7$ and $U(4)O_7$ bipyramids form a linear arrangement similar to the (UO_5) chain limited to four bipyramids, this four pyramids length chain is intersected at the ends by three bipyramids length chains U(3)U(4)U(2) forming eight bipyramids block which can be pictured by a capital **I** letter. Each block is linked by corner-sharing to six equivalent blocks to form the bi-dimensional arrangement (Fig. 5). This arrangement creates two kinds of sites, a five sides polygon which can be considered as the juxtaposition of a square and a triangle, the square is occupied by a square tetragonal $W(1)O_5$, and a larger I shaped hole which can be decomposed in three squares and four triangles, two squares are occupied by very

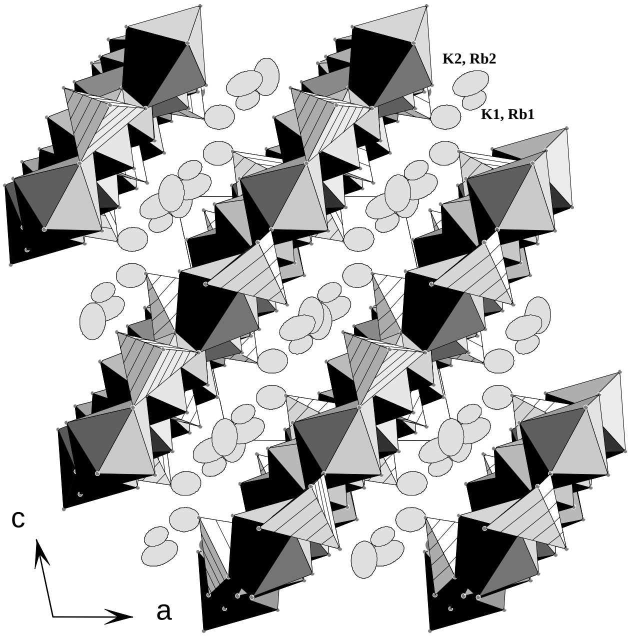

Fig. 6. The staking of the $(U_2WO_{10})^{2-}$ layers in the $M_2(UO_2)_2(WO_5)O$ [M=K (**3**), Rb (**4**)] compounds with the M^+ ions in the interspace.

distorted tetragonal pyramids $W(2)O_5$. The $W(1)O_5$ square pyramid is linked by edge-sharing to three UO_7 polyhedra from three different U_8O_{40} blocks. The $W(2)O_5$ tetragonal pyramid is linked by edge-sharing to one UO_7 polyhedron of one U_8O_{40} block and by corner-sharing to two UO_7 polyhedra, one of the same U_8O_{40} block and the second of an other block. So the tetragonal pyramids $W(1)O_5$ and $W(2)O_5$ are connected to two and three U_8O_{40} blocks, respectively. The arrangement of UO_7 and WO_5 polyhedra leads to layers $(U_4W_2O_{20})^{4-}$ parallel to $(10\bar{1})$ (Fig. 6). The K or Rb cations lie in the interspace and insure the cohesion of the structure.

In compounds **3** and **4**, the four independent uranium atoms are bonded to two oxygen atoms at short distances with an average U–O bond distance in the range 1.79–1.84 and 1.75–1.78 Å for the potassium and rubidium compounds, respectively, to form nearly linear uranyl ions UO_2^{2+}. Each uranyl ion is surrounded in the equatorial plane by a pentagonal environment of oxygen atoms that are situated at an average distance in the range from 2.34 to 2.35 Å for the both compounds forming a pentagonal bipyramidal coordination $(UO_2)O_5$ which represents the most common environment of U^{6+} ions. The two independent W(1) and W(2) tungsten atoms are coordinated by five oxygen atoms to form a square pyramidal environment with average distances $\langle W\text{–}O \rangle \cong 1.85$ Å for both compounds and apical oxygen atoms [O(9) and O(10)] situated at shorter distances, 1.71 and 1.78 Å for $K_2(UO_2)_2(WO_5)O$ (**3**), and 1.70 and 1.77 Å for the rubidium compound **4**.

Table 7
Selected bond distances (Å) and bond valences for $K_2(UO_2)_2(WO_5)O$ (**3**)

Atom	Distance	s_{ij}	Atom	Distance	s_{ij}
U1–O2	1.827(25)	1.531	U2–O1	1.789(25)	1.653
U1–O6	1.857(29)	1.445	U2–O3	1.829(28)	1.531
U1–O15	2.241(20)	0.693	U2–O15	2.131(26)	0.859
U1–O12^{i}	2.322(22)	0.596	U2–O16	2.329(20)	0.584
U1–O13^{ii}	2.318(21)	0.596	U2–O7	2.372(23)	0.538
U1–O16	2.381(27)	0.531	U2–O14	2.393(22)	0.52
U1–O13	2.439(23)	0.473	U2–O18^{iv}	2.460(21)	0.455
Σs_{ij}		*5.865*	Σs_{ij}		*6.14*
U3–O8	1.770(29)	1.718	U4–O4	1.792(29)	1.653
U3–O11	1.813(29)	1.591	U4–O5	1.799(29)	1.653
U3–O12	2.206(23)	0.736	U4–O15	2.194(24)	0.765
U3–O19^{v}	2.236(21)	0.695	U4–O12^{i}	2.314(20)	0.601
U3–O20	2.394(25)	0.52	U4–O14^{iv}	2.331(20)	0.584
U3–O17	2.432(21)	0.482	U4–O17^{i}	2.340(27)	0.573
U3–O7	2.485(22)	0.434	U4–O18^{iv}	2.557(22)	0.373
Σs_{ij}		*6.176*	Σs_{ij}		*6.204*
W1–O9	1.710(29)	1.75	W2–O20	1.795(23)	1.41
W1–O17	1.817(23)	1.3	W2–O10	1.782(29)	1.448
W1–O18	1.841(21)	1.231	W2–O19	1.841(21)	1.231
W1–O7	1.892(20)	1.073	W2–O13	1.880(25)	1.105
W1–O14	1.916(25)	0.992	W2–O16	1.934(22)	0.965
Σs_{ij}		*6.346*	Σs_{ij}		*6.159*
K1–O10	2.673(26)	0.234	K3–O10	2.703(27)	0.215
K1–O5^{x}	2.721(25)	0.204	K3–O2^{ix}	2.748(21)	0.193
K1–O6^{x}	2.738(26)	0.193	K3–O10^{ix}	2.894(27)	0.129
K1–O1	2.796(20)	0.164	K3–O20^{v}	2.909(27)	0.122
K1–O11^{xi}	2.878(28)	0.136	K3–O19	2.929(30)	0.116
K1–O8	2.990(26)	0.098	K3–O6^{x}	2.989(26)	0.098
K1–O9	3.017(24)	0.091	K3–O11^{v}	3.029(26)	0.088
K1–O7	3.084(28)	0.077	K3–O8	3.382(23)	0.034
Σs_{ij}		*1.197*	Σs_{ij}		*0.995*
K2–O9	2.764(28)	0.193	K4–O3	2.647(24)	0.247
K2–O5^{xii}	2.768(27)	0.183	K4–O2^{vii}	2.720(25)	0.204
K2–O1^{viii}	2.862(21)	0.178	K4–O4^{vii}	2.713(23)	0.21
K2–O4^{vi}	2.931(23)	0.14	K4–O8^{iii}	2.856(29)	0.144
K2–O14^{viii}	3.147(30)	0.116	K4–O6	3.004(27)	0.096
K2–O14^{viii}	3.147(30)	0.064	K4–O16	3.229(32)	0.051
Σs_{ij}		*0.874*	Σs_{ij}		*0.952*

Symmetry codes: (i) $-1+x, y, -1+z$; (ii) $1-x, -y, 2-z$; (iii) $x, y, -1+z$; (iv) $-0.5+x, 0.5-y, -0.5+z$; (v) $2-x, -y, 3-z$; (vi) $1+x, y, 1+z$; (vii) $1+x, y, z$; (viii) $0.5+x, 0.5-y, 0.5+z$; (ix) $1-x, -y, 3-z$; (x) $x, y, 1+z$; (xi) $-1+x, y, z$; (xii) $0.5+x, 0.5-y, 1.5+z$.

Selected bond lengths and bond valences for **3** and **4** are given in Tables 7 and 8. The average bond valence sums calculations for U, W and K/Rb atoms provide values of 6.086, 6.252, 1.005 and 6.311, 6.062, 1.034 for potassium and rubidium compounds, respectively. For the oxygen atoms the calculated valence bond sums range from 1.842 to 2.355 and 1.948 to 2.277 with an average valence bond of 2.045 and 2.075, for $K_2(UO_2)_2(WO_5)O$ and $Rb_2(UO_2)_2(WO_5)O$, respectively.

$Na_{10}(UO_2)_2(W_2O_{10})(WO_4)O$ (**5**). The structure of **5** is built from UO_7 pentagonal bipyramids, WO_6 octahedra and WO_4 tetrahedra. The $U(1)O_7$ distorted pentagonal bipyramids share two opposite edges with two others $U(1)O_7$ polyhedra to form the (UO_5) chain described for

Table 8
Selected bond distances (Å) and bond valences for $Rb_2(UO_2)_2(WO_5)O$ (**4**)

Atom	Distance	s_{ij}	Atom	Distance	s_{ij}
U1–O2	1.782(30)	1.686	U2–O1	1.762(29)	1.752
U1–O6	1.784(35)	1.686	U2–O3	1.800(29)	1.622
U1–O15	2.247(23)	0.682	U2–O15	2.130(26)	0.859
U1–O13^{i}	2.340(26)	0.573	U2–O16	2.345(23)	0.573
U1–O12	2.346(24)	0.573	U2–O14	2.367(24)	0.541
U1–O13	2.384(26)	0.531	U2–O7	2.400(26)	0.51
U1–O16	2.408(26)	0.501	U2–O18^{iii}	2.483(24)	0.438
Σs_{ij}		*6.232*	Σs_{ij}		*6.295*
U3–O11	1.757(30)	1.752	U4–O5	1.753(30)	1.786
U3–O8	1.792(30)	1.653	U4–O4	1.748(30)	1.786
U3–O12	2.225(26)	0.708	U4–O15	2.211(24)	0.736
U3–O19^{i}	2.272(25)	0.656	U4–O12	2.298(21)	0.619
U3–O20^{vi}	2.345(26)	0.573	U4–O17^{vi}	2.331(26)	0.584
U3–O17^{vi}	2.436(23)	0.473	U4–O14^{iii}	2.362(23)	0.551
U3–O7^{vi}	2.488(24)	0.429	U4–O18^{iii}	2.506(25)	0.413
Σs_{ij}		*6.244*	Σs_{ij}		*6.475*
W1–O9	1.699(30)	1.798	W2–O10	1.768(34)	1.488
W1–O17	1.872(24)	1.135	W2–O20	1.808(24)	1.335
W1–O7	1.875(24)	1.135	W2–O19	1.837(26)	1.231
W1–O18	1.888(23)	1.076	W2–O13	1.911(26)	1.019
W1–O14	1.923(25)	0.992	W2–O16	1.944(24)	0.915
Σs_{ij}		*6.136*	Σs_{ij}		*5.988*
Rb1–O10^{vii}	2.813(28)	0.228	Rb3–O2	2.859(29)	0.194
Rb1–O6	2.887(28)	0.184	Rb3–O10	2.878(32)	0.189
Rb1–O5	2.925(25)	0.165	Rb3–O10^{x}	2.907(27)	0.174
Rb1–O1^{vii}	2.944(28)	0.156	Rb3–O19^{x}	3.024(30)	0.129
Rb1–O11	2.947(25)	0.156	Rb3–O20^{ii}	3.037(28)	0.122
Rb1–O9^{vii}	2.971(26)	0.148	Rb3–O11^{iv}	3.225(25)	0.073
Rb1–O8^{xi}	3.080(25)	0.084	Rb3–O6^{i}	3.232(30)	0.073
Rb1–O7^{vii}	3.177(30)	0.077	Rb3–O8^{xiii}	3.246(24)	0.069
Σs_{ij}		*1.308*	Σs_{ij}		*0.834*
Rb2–O3^{xii}	2.882(26)	0.198	Rb4–O2^{xi}	2.918(25)	0.169
Rb2–O9^{iii}	2.913(28)	0.174	Rb4–O4^{xi}	2.845(26)	0.21
Rb2–O5^{iv}	2.935(27)	0.165	Rb4–O3	2.810(27)	0.228
Rb2–O1	3.025(27)	0.126	Rb4–O8^{xi}	3.063(29)	0.116
Rb2–O4^{viii}	3.244(25)	0.071	Rb4–O6	2.934(32)	0.16
Rb2–O14	3.394(29)	0.046	Rb4–O12^{xi}	3.835(32)	0.014
Rb2–O18^{ii}	3.511(29)	0.034	Rb4–O16	3.233(31)	0.073
Rb2–O9	3.573(28)	0.019			
Σs_{ij}		*1.023*	Σs_{ij}		*0.97*

Symmetry codes: (i) $1-x,-y,2-z$; (ii) $-1+x,y,z$; (iii) $-0.5+x,0.5-y,-0.5+z$; (iv) $x,y,1+z$; (v) $0.5+x,0.5-y,-0.5+z$; (vi) $-1+x,y,-1+z$; (vii) $x,y,-1+z$; (viii) $0.5+x,0.5-y,0.5+z$; (ix) $1+x,y,1+z$; (x) $1-x,-y,3-z$; (xi) $1+x,y,z$; (xii) $-0.5+x,0.5-y,0.5+z$; (xiii) $-x,-y,2-z$.

Table 9
Selected bond distances (Å) and bond valences for $Na_{10}(UO_2)_8(W_5O_{20})O_8$ (**5**)

Atom	Distance	s_{ij}	Atom	Distance	s_{ij}
U1–O2	1.840(9)	1.499	U2–O6	1.799(8)	1.625
U1–O3	1.847(9)	1.482	U2–O11	1.823(8)	1.552
U1–O13	2.192(8)	0.762	U2–O13^{v}	2.191(7)	0.764
U1–O12^{i}	2.209(8)	0.738	U2–O12	2.211(8)	0.733
U1–O12	2.215(9)	0.729	U2–O21^{v}	2.356(7)	0.557
U1–O4	2.356(7)	0.556	U2–O7	2.386(7)	0.524
U1–O13^{ii}	2.587(7)	0.355	U2–O4	2.531(9)	0.397
Σs_{ij}		*6.121*	Σs_{ij}		*6.152*
U3–O8	1.844(8)	1.49	U4–O9	1.792(9)	1.65
U3–O10	1.849(9)	1.473	U4–O5	1.815(9)	1.573
U3–O16	2.189(7)	0.768	U4–O16^{vii}	2.198(7)	0.752
U3–O16^{vii}	2.192(7)	0.762	U4–O20^{ix}	2.200(7)	0.75
U3–O20	2.196(6)	0.756	U4–O15^{ix}	2.375(7)	0.536
U3–O19	2.380(7)	0.532	U4–O1	2.387(7)	0.522
U3–O20^{vii}	2.552(7)	0.381	U4–O19	2.501(7)	0.42
Σs_{ij}		*6.162*	Σs_{ij}		*6.203*
Na1–O17^{iv}	2.44(2)	0.179	Na4–O10	2.480(19)	0.16
Na1–O3^{iv}	2.514(20)	0.146	Na4–O3^{xiii}	2.502(30)	0.151
Na1–O22	2.516(17)	0.146	Na4–O10^{vii}	2.570(31)	0.126
Na1–O10	2.532(18)	0.136	Na4–O3^{iv}	2.579(18)	0.123
Na1–O5	2.550(32)	0.133	Na4–O11^{xiii}	2.624(18)	0.109
Na1–O11^{vi}	2.592(32)	0.119	Na4–O12^{xiii}	2.697(11)	0.09
Na1–O19	3.006(20)	0.039	Na4–O5^{viii}	2.706(21)	0.087
Σs_{ij}		*0.901*	Σs_{ij}		*0.846*
Na2–O6^{x}	2.334(30)	0.238	Na3–O2^{ii}	2.461(21)	0.169
Na2–O6	2.334(30)	0.238	Na3–O2^{xi}	2.461(21)	0.169
Na2–O2^{x}	2.513(20)	0.147	Na3–O6^{xii}	2.538(24)	0.137
Na2–O2	2.513(20)	0.147	Na3–O6	2.538(24)	0.137
Na2–O18^{x}	2.719(15)	0.084	Na3–O2^{v}	2.696(32)	0.09
Na2–O18	2.719(15)	0.084	Na3–O2^{x}	2.696(32)	0.09
Na2–O4^{x}	2.898(22)	0.052	Na3–O13^{x}	2.971(12)	0.042
Na2–O4	2.898(22)	0.052	Na3–O13^{v}	2.971(12)	0.042
Σs_{ij}		*1.042*	Σs_{ij}		*0.876*
Na5–O9	2.374(33)	0.214	Na6–O8^{xiv}	2.523(17)	0.142
Na5–O9^{x}	2.374(33)	0.214	Na6–O8^{vii}	2.523(17)	0.142
Na5–O8^{x}	2.415(18)	0.192	Na6–O9^{xv}	2.590(21)	0.119
Na5–O8	2.415(18)	0.192	Na6–O9	2.590(21)	0.119
Na5–O14^{x}	2.617(14)	0.111	Na6–O8^{x}	2.654(35)	0.1
Na5–O14	2.617(14)	0.111	Na6–O8^{ix}	2.654(35)	0.1
Σs_{ij}		*1.034*	Σs_{ij}		*0.722*
Na7–O22	2.341(12)	0.234			
Na7–O17	2.362(32)	0.22			
Na7–O5^{iv}	2.377(17)	0.211			
Na7–O22^{vi}	2.642(25)	0.104			
Na7–O11	2.682(25)	0.093			
Σs_{ij}		*0.862*			
W1–O17	1.743(8)	1.605	W2–O22	1.742(8)	1.6
W1–O21	1.754(11)	1.554	W2–O15	1.764(12)	1.512
W1–O4	1.866(8)	1.148	W2–O19	1.864(7)	1.151
W1–O1	1.926(7)	0.981	W2–O7	1.912(7)	1.016
W1–O7	2.202(8)	0.463	W2–O1	2.194(8)	0.473
W1–O18	2.243(13)	0.415	W2–O14	2.250(7)	0.408
Σs_{ij}		*6.161*	Σs_{ij}		*6.16*
W3–O18^{x}	1.755(20)	1.545			
W3–O18	1.755(20)	1.545			
W3–O14	1.766(17)	1.5			
W3–O14^{x}	1.766(17)	1.5			
Σs_{ij}		*6.09*			

Symmetry codes: (i) $x,1-y,0.5+z$; (ii) $x,1-y,-0.5+z$; (iii) $0.5-x,0.5+y,1.5-z$; (iv) $0.5-x,0.5-y,2-z$; (v) $x,y,-1+z$; (vi) $0.5-x,0.5-y,1-z$; (vii) $x,-y,0.5+z$; (viii) $x,-y,-0.5+z$; (ix) $x,y,1+z$; (x) $-x,y,1.5-z$; (xi) $-x,1-y,1-z$; (xii) $-x,y,0.5-z$; (xiii) $0.5-x,-0.5+y,1.5-z$; (xiv) $-x,-y,2-z$; (xv) $-x,y,2.5-z$.

compound **2**. This chain runs down the *c*-axis. The $U(2)O_7$ pentagonal bipyramids are linked by edge-sharing on both sides of the chain to form a three bipyramids wide ribbon running down the *c*-axis. A similar but crystallographically independent ribbon is formed from polyhedra around U(3) and U(4). The interior (UO_5) chains of the ribbons $(U(1)U(2)O_9)$ and $(U(3)U(4)O_9)$ are located at about $y = 0.5$ and 0.0, respectively (Fig. 7). Similar one-dimensional three polyhedra wide ribbons built from edge-sharing distorted pentagonal bipyramids have been described in the

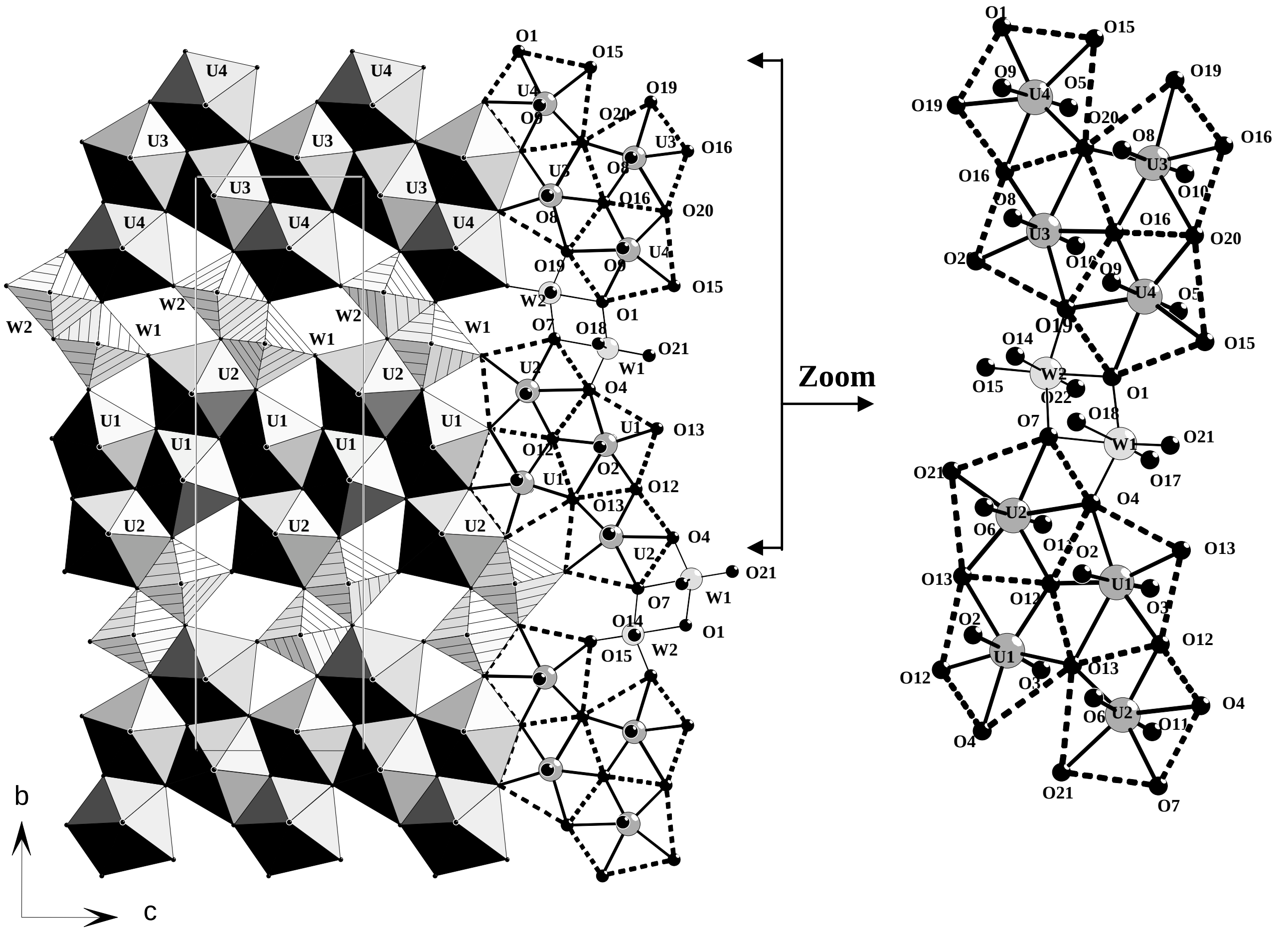

Fig. 7. Projection of the layer $(U_4W_2O_{22})^{8-}$ along the *a*-axis of $Na_{10}U_8W_5O_{44}$ compound (**5**) showing the connection between three polyhedra wide ribbons consisting of edge-sharing UO_7 pentagonal bipyramids and W_2O_{10} units consisting of two edge-sharing octahedra.

uranyl iodates *AE*$[(UO_2)_2(IO_3)_2](H_2O)$ (*AE* = Sr, Pb) [14]. The $W(1)O_6$ and $W(2)O_6$ octahedra share an O(1)–O(7) edge to form a W_2O_{10} dimeric unit. The W_2O_{10} units link two parallel (U_2O_9) ribbons by sharing an edge and a corner with two $U(2)O_7$ pentagonal bipyramids of one ribbon and with two $U(4)O_7$ pentagonal bipyramids of the parallel ribbon resulting in layers parallel to (100). The unit cell contains four layers at $x \approx 0.125$, 0.375, 0.625, 0.875, respectively. The layers on both sides of $x = 0.0$ and 0.5 are linked by WO_4 tetrahedra resulting in pillared double layers or "sandwiches" $(U_8W_5O_{44})^{10-}$, Fig. 8. The double layers sheets are stacked along the [100] direction and are separated by Na^+ ions. The other Na^+ ions are located in the rectangular tunnels running down the *c*-axis within the pillared double layers. A WO_4 tetrahedron, that acts as a pillar in the linkage of two layers, shares its four corners with two W_2O_{10} unit formed from edge-shared WO_6 octahedra, resulting in penta-nuclear anion $W_5O_{20}^{10-}$ (Fig. 9).

Selected interatomic distances and bond valences for compound **5** are given in Table 9. Astonishingly, the U = O bond lengths of the U atoms that belong to the (UO_5) chains (average ⟨U = O⟩ = 1.843 Å for U(1) and 1.846 Å for U(3)) are longer than the corresponding bonds for the other U atoms (average ⟨U = O⟩ = 1.811 Å for U(2) and 1.804 Å for U(3)) that are in expected ranges for uranyl ions. However, similar and even higher U = O distances have already been observed, for example, in $Ca_{12}[(UO_2)(CO_3)_3]_4Cl_8(H_2O)_{47}$ [44] (U–O(2) = 1.84(1)) Å and in uranopilite [45] with (U(1)–O(1) = 1.87(2)). In the equatorial plane the U–O distances show significant variations with values ranging from 2.189 to 2.587 Å, the long distances are with oxygen atoms from WO_6 octahedra and the shortest with the oxide atoms shared between three UO_7 polyhedra. However, the average U–O equatorial distances for each U atom (2.312, 2.335, 2.302, and 2.332 Å for U(1), U(2), U(3), and U(4), respectively) are in good agreement with the value obtained for U atoms in pentagonal bipyramidal environment [40].

The WO_6 octahedra are highly distorted as in $K_2(UO_2)(W_2O_8)$ with W–O distances ranging from 1.743 to 2.243 Å for W(1) and from 1.742 to 2.250 Å for W(2), the longest bonds are with oxygen that are shared with a WO_4 tetrahedron. In the W(1)–O(7)–W(2)–O(1)

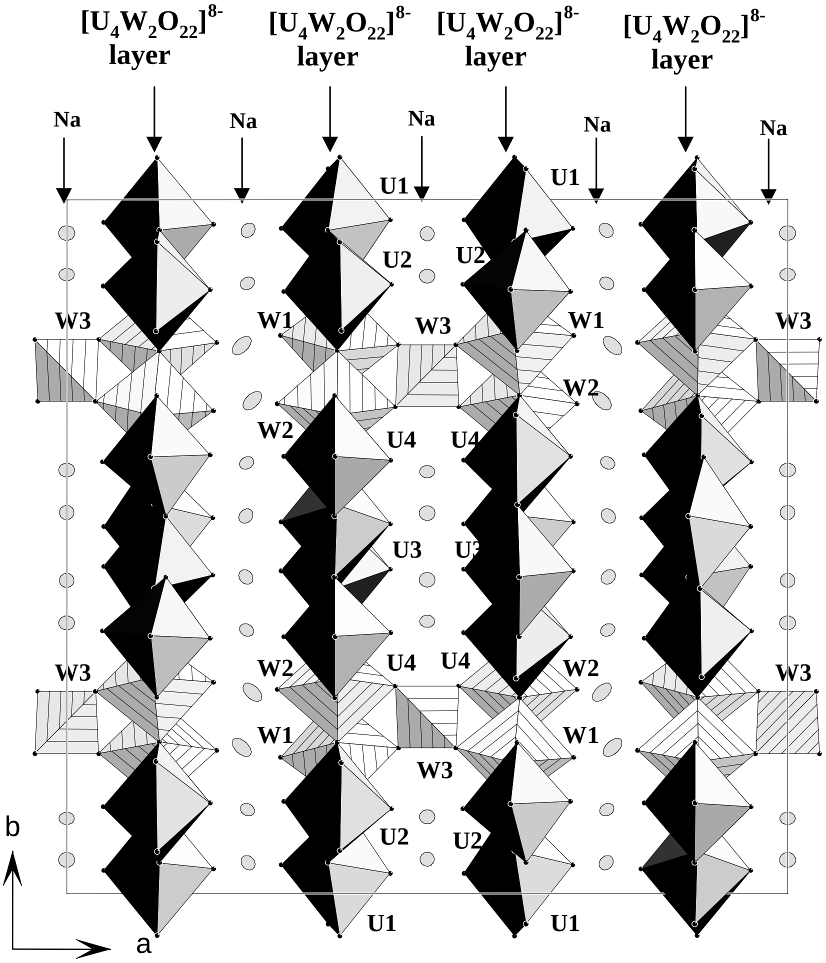

Fig. 8. Projection of the structure of $Na_{10}U_8W_5O_{44}$ (**5**) along **c**-axis showing the connection of two consecutive $(U_4W_2O_{22})^{8-}$ layers by WO_4 tetrahedra to form a sheet of pillared double layers and the Na^+ ions in the rectangular tunnel and in the interlayer between sheets.

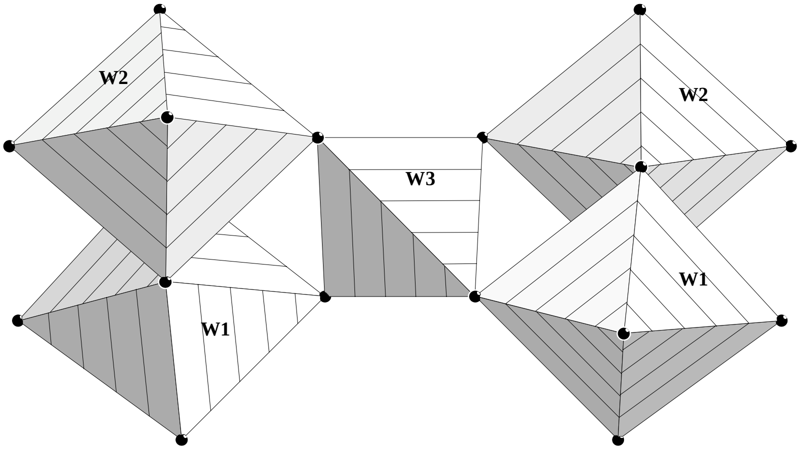

Fig. 9. The (W_2O_{20}) polyanion formed by two W_2O_{10} units consisting of edge-sharing octahedra connected by a WO_4 tetrahedron.

ring short and long distances alternate. The WO_4 tetrahedron is nearly regular with an average W–O distance (1.76 Å) in good accordance with the sum $^{IV}r(W^{6+}) + {}^{IV}r(O^{2-}) = 1.80$ Å [46].

Bond valence sums calculations provide average values of 6.159 and 6.137 for U and W atoms, respectively. For the sodium atoms the calculated valence bond sums range from 0.722 to 1.041 and for oxygen atoms from 1.873 to 2.290, with average values of 0.898 and 2.021 for sodium and oxygen atoms, respectively.

4. Conclusion

In the studied uranyl compounds, uranium is systematically in a pentagonal bipyramidal environment with two short U=O bonds and five longer equatorial distances. The pentagonal bipyramids share equatorial edges to form various arrangements: (i) one polyhedron wide chains in compounds **1** and **2**, (ii) bi-dimensional network in compounds **3** and **4** and (iii) three polyhedra wide ribbons in compound **5**. In compounds **1**, **2**, and **5**, the chains or ribbons are linked by WO_6 octahedra, two WO_6 octahedra forming a W_2O_{10} dimmer by edge-sharing, resulting uranium tungsten oxides layers. In compounds **3** and **4**, the sites created by the UO_7 arrangement are occupied by distorted WO_5 square pyramids.

In compounds **1**, **2**, **3**, and **4**, the uranium tungsten layers are separated by the alkali ions. In compound **5**, two consecutive layers are pillared by WO_4 tetrahedra resulting in the formation of sheets of two layers thickness. Two types of Na^+ ions occupy the rectangular tunnels within the sheets and the inter-sheet space, respectively. Substitution or exchange of these two types of Na^+ ions are plane, the study of the mobility of intra-tunnel and inter-sheet species would be interesting.

References

[1] F. Abraham, C. Dion, M. Saadi, J. Mater. Chem. 3 (5) (1993) 459.
[2] F. Abraham, C. Dion, N. Tancret, M. Saadi, Adv. Mater. Res. 1–2 (1994) 511.
[3] I. Dubribreux, C. Dion, F. Abraham, M. Saadi, J. Solid State Chem. 146 (1999) 258.
[4] C. Dion, S. Obbade, E. Rackelboom, M. Saadi, F. Abraham, J. Solid State Chem. 155 (2000) 342.
[5] I. Dubribreux, M. Saadi, S. Obbade, C. Dion, F. Abraham, J. Solid State Chem. (2002), in press.
[6] M. Gasperin, J. Solid State Chem. 67 (1987) 219.
[7] M. Gasperin, Acta Crystallogr. C 43 (1987) 404.
[8] N.G. Chernorukov, E.V. Suleimanov, N.P. Egorov, I.M. Romanenko, Russ. J. Gen. Chem. 64 (1) (1994) 1.
[9] C. Dion, S. Obbade, E. Raekelboom, F. Abraham, M. Saadi, J. Solid State Chem. 155 (2000) 342.
[10] S. Obbade, C. Dion, M. Saadi, F. Abraham, 31èmes Journées des Actinides, Saint-Malo, France, 26–28 April, 2001, extended abstracts, O7 and P5.
[11] S.V. Krivovichev, P.C. Burns, Can. Mineral. 39 (2001) 197.
[12] S.V. Krivovichev, P.C. Burns, Can. Mineral. 39 (2001) 207.
[13] P.A. Tanner, T.C.W. Mak, Inorg. Chem. 38 (1999) 6024.
[14] A.C. Bean, T.E. Albrecht-Schmitt, J. Solid State Chem. 161 (2001) 416.
[15] A.J. Guesdon, J. Chardon, J. Provost, B. Raveau, Solid State Chem. 165 (2002) 89.
[16] A.J. Locok, P.C. Burns, J. Solid State Chem. 163 (2002) 275.
[17] L.A. Hayden, P.C. Burns, J. Solid State Chem. 163 (2002) 313.
[18] Y. Li, P.C. Burns, J. Solid State Chem. 166 (2002) 219.
[19] M. Pham-Thi, Ph. Colomban, Solid State Ionics 17 (1985) 295.
[20] A.N. Fitch, M. Cole, Mater. Res. Bull. 26 (1991) 407.
[21] M. Pham-Thi, Rh. Adet, G. velasco, Appl. Phys. Lett. 48 (1986) 1348.
[22] J. Benavente, J.R. ramos-Barrado, M. Martinez, S. Bruque, J. Appl. Electrochem. 25 (1995) 68.
[23] G.M. Sheldrick, SAINT Plus version 5.00, Bruker Analytical X-ray Systems, Madison, WI, 1998.
[24] G.M. Sheldrick, SHELXTL NT, Program Suite for solution and Refinement of Crystal Structure, Version 5.1, Bruker Analytical X-ray Systems, Madison, WI, 1998.
[25] G.M. Sheldrick, SADABS: Program for absorption correction using SMART CCD based on the method of Blessing: blessing, R. H., Acta Crystallogr. A 51 (1995) 33.
[26] G. Smith, R.J. Snyder, J. Appl. Crystallogr. 12 (1979) 60.
[27] G.M. Sheldrick, Acta Crystallogr. A 46 (1990) 467.
[28] P.G. Dickens, G.P. Stuttard, J. Mater. Chem. 2 (1992) 691.
[29] M. Gasperin, R. Chevalier, Bull. Soc. Fr. Mineral. Cristallogr. 93 (1970) 18.
[30] L.M. Kovba, Radiokhimiya (English Translation) 13 (1971) 940.
[31] P.G. Dickens, C.P. Stuttard, R.G.J. Ball, A.V. Powell, S. Hull, S. Patat, J. Mater. Chem. 2 (1992) 161.
[32] N. Tancret, S. Obbade, F. Abraham, Eur. J. Solid State Inorg. Chem. 32 (1995) 195.
[33] A.M. Chippindale, P.J. Dickens, G.J. Flynnand, G.P. Stuttard, J. Mater. Chem. 5 (1) (1995) 141.
[34] M. Saadi, C. Dion, F. Abraham, J. Solid State Chem. 150 (2000) 72.
[35] J. Locock, P.C. Burns, J. Solid State Chem. 163 (2002) 275.
[36] P. Benard, D. Loüer, N. Dacheux, V. Brandel, M. Genet, Chem. Mater. 6 (1994) 1049.
[37] T.LC remers, P.G. Eller, R.A. Penneman, C.C. Herrick, Acta Crystallogr. 39 (1983) 1163.
[38] B.O. Loopstra, Acta Crystallogr. 17 (1964) 651.
[39] S. Obbade, M. Saadi, L. Duvieubourg, C. Dion, F. Abraham, J. Solid State Chem. (2002), in press.
[40] P.C. Burns, M.L. Miller, R.C. Ewing, Can. Mineral. 35 (1996) 845.
[41] P.C. Burns, R. Finch (Eds.), Rev. Miner. 38 (1999) 23.
[42] P.C. Burns, R.C. Ewing, F.C. Hawthorne, Can. Mineral. 35 (1997) 1551.
[43] I.D. Brown, D. Altermatt, Acta Crystallogr. B 41 (1985) 244.
[44] Y. Li, P.C. Burns, J. Solid State Chem. 166 (2002) 219.
[45] P.C. Burns, Can. Mineral. 39 (2001) 1139.
[46] R.D. Shannon, Acta Crystallogr. A 32 (1976) 751.